

SPEEDING UP AN UNSTEADY FLOW SIMULATION BY ADAPTIVE BDDC AND KRYLOV SUBSPACE RECYCLING

MARTIN HANEK^{†*}, JAN PAPEŽ[†], AND JAKUB ŠÍSTEK[†]

Abstract. We deal with accelerating the solution of a sequence of large linear systems solved by an iterative Krylov subspace method. The sequence originates from time-stepping within a simulation of an unsteady incompressible flow. We apply a pressure correction scheme, and we focus on the solution of the Poisson problem for the pressure corrector. Its scalable solution presents the main computational challenge in many applications. The right-hand side of the problem changes in each time step, while the system matrix is constant and symmetric positive definite. The acceleration techniques are studied on a particular problem of flow around a unit sphere. Our baseline approach is based on a parallel solution of each problem in the sequence by nonoverlapping domain decomposition method. The interface problem is solved by the preconditioned conjugate gradient (PCG) method with the three-level BDDC preconditioner. Three techniques for accelerating the solution are gradually added to the baseline approach. First, the stopping criterion for the PCG iterations is studied. Next, deflation is used within the conjugate gradient method with several approaches to Krylov subspace recycling. Finally, we add the adaptive selection of the coarse space within the three-level BDDC method. The paper is rich in experiments with careful measurements of computational times on a parallel supercomputer. The combination of the acceleration techniques eventually leads to saving about one half of the computational time.

Key words. Navier-Stokes equations, pressure correction, domain decomposition, stopping criteria, adaptive BDDC, deflated PCG, Krylov subspace recycling

AMS subject classifications. 65N55, 65Y05, 76D05

1. Introduction. We study the problem of solving a sequence of linear systems with a constant matrix and a number of right-hand sides. There are many scenarios resulting in such sequences, and we apply and study the methods on the Poisson problem of pressure (corrector) within an unsteady simulation of an incompressible flow.

Unsteady incompressible flows of Newtonian fluids are modelled by the Navier-Stokes equations. The system is time-dependent and nonlinear, and in its generality, it leads to solving a system of nonlinear equations repeatedly in each time step. This approach can be very demanding with respect to computational resources, and a number of widely used numerical schemes circumvent the need to solve these systems by splitting the whole problem into solving a sequence of simpler problems within each time step. Let us mention the Pressure Implicit with Splitting of Operator (PISO) scheme [13], implicit-explicit (IMEX) time integration [14], or the pressure-correction methods (see, e.g., the review in [10]), to name a few. In these approaches, a Poisson-type problem for pressure typically becomes the most time-consuming problem to solve, and this trend worsens with the problem size, see, e.g., [23]. This is the reason why a considerable attention has been devoted to accelerating the Poisson-type problems in this context in literature (e.g., [3, 4, 5, 9, 19]). To solve the problem in parallel, multigrid methods, preconditioned Krylov subspace methods, and combination thereof are often employed (see, e.g., [28]).

Somewhat less common is using domain decomposition solvers in this context. We investigated the applicability of a nonoverlapping domain decomposition method,

^{*}Faculty of Mechanical Engineering, Czech Technical University in Prague, Czech Republic (martin.hanek@fs.cvut.cz).

[†]Institute of Mathematics of the Czech Academy of Sciences, Prague, Czech Republic (papez@math.cas.cz, sistek@math.cas.cz).

namely the Balancing Domain Decomposition based on Constrains (BDDC) preconditioner, for this task in [11]. It provides the baseline approach also for the present paper. More specifically, we use the three-level BDDC preconditioner [27] for the preconditioned conjugate gradient (PCG) method. Domain decomposition (DD) methods have a relatively expensive setup, which includes factorization of the local subdomain matrices, and the matrix of the coarse problem. It is then repeatedly used for each right-hand side in the time-stepping sequence. The DD method reduces a global problem to the interface among subdomains, and runs PCG on the Schur complement problem. This leads to a significant reduction of the size of the vectors in the Krylov method.

We apply the finite element method (FEM) in connection with the incremental pressure-correction method to discretize the problem. If the computational domain is fixed, the problems for the pressure corrector have a constant matrix and a new right-hand side vector in each time step. Hence, the interface Schur complement problem and the BDDC preconditioner are set up once in the first time step and reused in subsequent time steps.

In the rest of this section, we briefly review the techniques employed to accelerate the solution of the arising sequence of linear systems. The gradual improvements eventually led us to saving up to one half of the overall simulation time for realistic computations. The techniques are then described in more detail in the subsequent sections.

Stopping criterion for Krylov iterations. When solving a sequence of algebraic systems corresponding to time-dependent simulations with subsequent solutions close one to another, it seems appropriate to use the previously computed approximation as the starting guess for the current (new) system. This however may not bring a significant improvement in the solution time unless the stopping criterion is set properly, as we will discuss and illustrate in numerical experiments.

In this study we terminate the iterations of PCG after a sufficient reduction of the relative residual. However, we suggest to normalize the residual norm $\|\mathbf{r}_k\|$ (where $\mathbf{r}_k = \mathbf{b} - \mathbf{A}\mathbf{x}_k$ is the residual associated with the approximation \mathbf{x}_k from the k th iteration) by a quantity that is not related to the initial approximation. For that purpose, we take the norm of the right-hand side \mathbf{b} and terminate the iterations when

$$\frac{\|\mathbf{r}_k\|}{\|\mathbf{b}\|} < 10^{-6}.$$

We compare this approach with normalizing by the norm of the initial residual \mathbf{r}_0 , that is stopping when

$$\frac{\|\mathbf{r}_k\|}{\|\mathbf{r}_0\|} < 10^{-6}.$$

We show that the latter criterion does not reduce the number of iterations in case when a good initial approximation is available.

Krylov subspace recycling. Running the conjugate gradient (CG) method in a subspace defined as the orthogonal complement of a stored basis is an established approach known as deflated CG [8, 22]. Since Krylov subspace methods typically reduce oscillating component of the error faster than smooth components, making the Krylov subspace orthogonal to the eigenvectors corresponding to the smallest eigenvalues typically results in faster convergence. As such, deflation can be seen as an alternative to preconditioning (see, e.g., [25]). On the other hand, it requires

a careful implementation as some of the operations in the approach are sensitive to accumulation of rounding errors and numerical loss of orthogonality. Another drawback of these methods is the relatively high memory cost of storing the deflation basis which limits its size. Both of these issues are mitigated by the use of the BDDC preconditioner in our context.

Adaptive selection of constraints in BDDC. The BDDC preconditioner allows a flexible definition of its coarse space through defining the coarse degrees of freedom. There are several variants of the adaptive BDDC (see the overview papers [15, 21]), and the common feature of the methods is solving a number of local eigenvalue problems, followed by using selected eigenvectors for defining optimal coarse degrees of freedom. The enriched coarse space typically improves the convergence of the iterative method at the cost of more expensive preconditioner setup due to solving the eigenvalue problems. While these approaches were developed mostly for problems with heterogeneous materials with largely varying coefficients, they can be seen as a general approach to adjusting the strength of the preconditioner. Hence, they present an interesting option also for time-dependent problems studied in this paper, in which any reduction of the number of iterations can lead to large savings of the computational time needed for the whole sequence.

In our setting, we combine the adaptive BDDC preconditioner with deflated CG, so that we can benefit from synergy of these approaches in several aspects. Namely, the CG method runs on much shorter vectors (with the length given by the interface size rather than the global size) allowing storing more basis vectors of the deflation basis. A nonstandard feature of combining BDDC with deflated CG is that the spectrum of the preconditioned operator is bounded from below by 1 with many eigenvalues clustered near this value. This means that deflating eigenvectors corresponding to the smallest eigenvalues does not significantly improve the CG convergence. Instead, we use the eigenvectors corresponding to the *largest* eigenvalues of the preconditioned operator as the basis for deflation. This can be understood as another level of preconditioning, further reducing the upper bound of the spectrum of the preconditioned operator; see, e.g., [25].

In our case study (described in more details in Section 6) the proper choice of stopping criterion can save 14 % of the computational time spent on solving the system for pressure correction. When combined with a subspace deflation, this improvement is 28 %. Using adaptive coarse space with the proper stopping criterion saves 32 %. Finally, the combination of the proper stopping criterion, subspace deflation, and adaptive coarse space reduces the time by 36 %. The savings are even higher, over 50 %, in a larger tested problem.

2. Model problem. We consider a domain $\Omega \subset \mathbb{R}^3$ with its boundary $\partial\Omega$ consisting of three disjoint parts $\partial\Omega_S$, $\partial\Omega_\infty$, and $\partial\Omega_O$, $\partial\Omega = \partial\Omega_S \cup \partial\Omega_\infty \cup \partial\Omega_O$. Part $\partial\Omega_S$ is the interface between fluid and the rigid body, $\partial\Omega_\infty$ is the inflow free-stream boundary, and $\partial\Omega_O$ is the outflow boundary. The flow is governed by the Navier-Stokes equations of an incompressible viscous fluid,

$$(2.1) \quad \begin{aligned} \frac{\partial \mathbf{u}}{\partial t} + (\mathbf{u} \cdot \nabla) \mathbf{u} - \nu \Delta \mathbf{u} + \nabla p &= \mathbf{0} & \text{in } \Omega, \\ \nabla \cdot \mathbf{u} &= 0 & \text{in } \Omega, \end{aligned}$$

where \mathbf{u} is the velocity vector of the fluid, t denotes time, ν is the kinematic viscosity of the fluid, and p is the kinematic pressure. System (2.1) is complemented by the initial and boundary conditions: $\mathbf{u}(t = 0, \mathbf{x}) = \mathbf{0}$ in Ω , $\mathbf{u}(t, \mathbf{x}) = \mathbf{u}_\infty$ on $\partial\Omega_\infty$, $\mathbf{u}(t, \mathbf{x}) = \mathbf{0}$

on $\partial\Omega_S$, and $-\nu(\nabla\mathbf{u})\mathbf{n} + p\mathbf{n} = \mathbf{0}$ on $\partial\Omega_O$, with \mathbf{n} being the unit outer normal vector of $\partial\Omega$.

System (2.1) can be efficiently solved by a pressure-correction method. In particular, we use the incremental pressure-correction method in the *rotational form* discussed by [10]. Details of our implementation can be found in [23].

In this approach, we first define the pressure increment (corrector) $\psi^{(n+1)} = p^{(n+1)} - p^{(n)} + \nu\nabla \cdot \mathbf{u}^{(n+1)}$. In order to compute the velocity and pressure fields $(\mathbf{u}^{(n+1)}, p^{(n+1)})$ at time $t^{(n+1)}$, the following three subproblems are subsequently solved.

1. The velocity field $\mathbf{u}^{(n+1)}$ is obtained by solving the convection-diffusion problem for each component of velocity

$$(2.2) \quad \frac{1}{\Delta t} \mathbf{u}^{(n+1)} + (\mathbf{u}^{(n)} \cdot \nabla) \mathbf{u}^{(n+1)} - \nu \Delta \mathbf{u}^{(n+1)} = \frac{1}{\Delta t} \mathbf{u}^{(n)} - \nabla(p^{(n)} + \psi^{(n)}) \quad \text{in } \Omega$$

for $\mathbf{u}^{(n+1)} = \mathbf{u}_\infty$ on $\partial\Omega_\infty$, $\mathbf{u}^{(n+1)} = \mathbf{0}$ on $\partial\Omega_S$, and $\nu(\nabla\mathbf{u}^{(n+1)})\mathbf{n} = p^{(n)}\mathbf{n}$ on $\partial\Omega_O$.

2. Next, the pressure corrector $\psi^{(n+1)}$ is obtained by solving the Poisson problem

$$(2.3) \quad -\Delta\psi^{(n+1)} = -\frac{1}{\Delta t} \nabla \cdot \mathbf{u}^{(n+1)} \quad \text{in } \Omega$$

for $\frac{\partial\psi^{(n+1)}}{\partial\mathbf{n}} = 0$ on $\partial\Omega_\infty \cup \partial\Omega_S$ and $\psi^{(n+1)} = 0$ on $\partial\Omega_O$.

3. Finally, the pressure field $p^{(n+1)}$ is updated with

$$(2.4) \quad p^{(n+1)} = p^{(n)} + \psi^{(n+1)} - \nu\nabla \cdot \mathbf{u}^{(n+1)}.$$

Problems (2.2), (2.3), and (2.4) are discretized by the finite element method (FEM) using Taylor-Hood $Q_2 - Q_1$ hexahedral elements. They approximate the velocity and pressure fields by continuous piecewise tri-quadratic and tri-linear basis functions, respectively. In the finite element mesh, there are n_u nodes with velocity unknowns and n_p nodes with pressure unknowns, with the ratio n_u/n_p being approximately 8.

For solving the algebraic problems arising from (2.2) and (2.4), we use the methods identified as optimal by [23]. In particular, the Generalized Minimal Residual method (GMRES) is used for (2.2), and the PCG method for (2.4). Block Jacobi preconditioner using ILU(0) on the blocks corresponding to mesh partitions is used for both problems.

Problem (2.3) translates to an algebraic system with a discrete Laplacian matrix of size $n_p \times n_p$ which is symmetric and positive definite for $\partial\Omega_O \neq \emptyset$, i.e., a nonempty part with the ‘do-nothing’ boundary condition,

$$(2.5) \quad \mathbf{K} \mathbf{x}^{(n+1)} = \mathbf{f}^{(n+1)}.$$

This is a well-studied case from the point of view of domain decomposition methods, which are suitable solvers for this task. The main focus of this study is a scalable solution of (2.5) arising from the Poisson problem for pressure corrector (2.3).

3. BDDC method with adaptive coarse space. As the baseline approach to solve the sequence of problems (2.5), we employ the three-level version [27, 17] of the BDDC method [6] implemented in the BDDCML¹ library. In particular, the approach is

¹<https://users.math.cas.cz/~sistek/software/bddcml.html>

based on (i) reducing the global problem on the whole domain to the reduced problem defined at the interface between subdomains, (ii) solving the reduced problem using PCG, while (iii) preconditioning the problem by the BDDC preconditioner. For the sake of brevity, we drop the time index $(n + 1)$ in the following discussion. More precisely, vectors \mathbf{x} and \mathbf{f} without superscript are considered in the $(n + 1)$ -st time level, while the superscript (n) will be kept for their counterparts from the previous n -th time level.

3.1. Iterative substructuring. First, we consider the reduction of the global problem to the inter-subdomain interface. This procedure is rather standard and described, e.g., in monographs [7, 26]. To this end, the finite element mesh is divided into N_S nonoverlapping subdomains $\Omega_i, i = 1, \dots, N_S$, with the partition respecting inter-element boundaries. The subset of unknowns to which elements of subdomain Ω_i contribute to is called local subdomain unknowns. This construction splits the unknowns to those belonging to just one subdomain, called *interior* unknowns, and the unknowns shared by several subdomains, which form the *interface* Γ .

The first step in iterative substructuring is to reduce the global problem to the interface. For each local subdomain, we split the unknowns belonging to interior \mathbf{x}_i^I and the interface \mathbf{x}_i^Γ , which leads to a 2×2 blocking of the local linear system,

$$(3.1) \quad \begin{bmatrix} \mathbf{K}_i^{II} & \mathbf{K}_i^{I\Gamma} \\ \mathbf{K}_i^{\Gamma I} & \mathbf{K}_i^{\Gamma\Gamma} \end{bmatrix} \begin{bmatrix} \mathbf{x}_i^I \\ \mathbf{x}_i^\Gamma \end{bmatrix} = \begin{bmatrix} \mathbf{f}_i^I \\ \mathbf{f}_i^\Gamma \end{bmatrix}.$$

Here the local interface unknowns \mathbf{x}_i^Γ can be assembled into a global set of unknowns at the interface of all subdomains Γ utilising an interface restriction matrix $\mathbf{R}_i^\Gamma : \Gamma \rightarrow \Gamma_i$, where $\mathbf{x}^\Gamma = \sum_{i=1}^{N_S} (\mathbf{R}_i^\Gamma)^T \mathbf{x}_i^\Gamma$.

The iterative substructuring seeks the solution of the global interface problem

$$(3.2) \quad \mathbf{A} \mathbf{x}^\Gamma = \mathbf{b},$$

using, for instance, the PCG method. The global Schur complement matrix \mathbf{A} comprises of the subdomain contributions,

$$(3.3) \quad \mathbf{A} = \sum_{i=1}^{N_S} (\mathbf{R}_i^\Gamma)^T \mathbf{A}_i \mathbf{R}_i^\Gamma,$$

where the local Schur complement with respect to Γ_i is defined as

$$(3.4) \quad \mathbf{A}_i = \mathbf{K}_i^{\Gamma\Gamma} - \mathbf{K}_i^{\Gamma I} (\mathbf{K}_i^{II})^{-1} \mathbf{K}_i^{I\Gamma}.$$

Similarly, the right-hand side is assembled from the subdomain vectors

$$(3.5) \quad \mathbf{b} = \sum_{i=1}^{N_S} (\mathbf{R}_i^\Gamma)^T \mathbf{b}_i,$$

where

$$(3.6) \quad \mathbf{b}_i = \mathbf{f}_i^\Gamma - \mathbf{K}_i^{\Gamma I} (\mathbf{K}_i^{II})^{-1} \mathbf{f}_i^I.$$

Once we know the local solution at the interface \mathbf{x}_i^Γ , the solution in the interior of each subdomain \mathbf{x}_i^I is recovered from the first row of (3.1). Note that neither the global Schur complement matrix \mathbf{A} nor the local Schur complement matrices \mathbf{A}_i are explicitly constructed in the iterative substructuring, since only multiplications of vectors by matrices \mathbf{A}_i are needed at each PCG iteration.

3.2. Multilevel BDDC preconditioner. Multilevel BDDC preconditioner is used within PCG when solving the interface problem (3.2). More precisely, an action of the preconditioner \mathbf{M}_{BDDC}^{-1} produces a preconditioned residual \mathbf{z}^Γ from the residual in the k -th iteration $\mathbf{r}^\Gamma = \mathbf{A}\mathbf{x}_k^\Gamma - \mathbf{b}$ by implicitly solving the system $\mathbf{M}_{BDDC}\mathbf{z}^\Gamma = \mathbf{r}^\Gamma$.

In the construction of the BDDC preconditioner, a set of coarse degrees of freedom required to be continuous among subdomains is selected. If enough coarse degrees of freedom are defined for each subdomain, the preconditioner corresponds to an invertible matrix. In the baseline approach, we consider function values at selected interface nodes (corners) and arithmetic averages across subdomain faces and edges as the coarse degrees of freedom. In adaptive BDDC, we further enrich this set by weighted averages over faces of subdomains derived from eigenvectors of generalized eigenvalue problems for each pair of subdomains sharing a face. This approach is described in Section 3.3.

In the standard 2-level BDDC method, the coarse degrees of freedom define a global coarse problem with the unknowns \mathbf{u}_C and local subdomain problems with mutually independent degrees of freedom \mathbf{u}_i .

The BDDC method provides an approximate solution by combining the global coarse and local subdomain components as

$$(3.7) \quad \mathbf{z}^\Gamma = \sum_{i=1}^{N_S} (\mathbf{R}_i^\Gamma)^T \mathbf{D}_i \mathbf{R}_{Bi} (\mathbf{u}_i + \Phi_i \mathbf{R}_{Ci} \mathbf{u}_C).$$

Vectors \mathbf{u}_C and \mathbf{u}_i are obtained in each iteration by solving

$$(3.8) \quad \mathbf{K}_C \mathbf{u}_C = \sum_{i=1}^{N_S} \mathbf{R}_{Ci}^T \Phi_i^T \mathbf{R}_{Bi}^T \mathbf{D}_i \mathbf{R}_i^\Gamma \mathbf{r}^\Gamma,$$

$$(3.9) \quad \begin{bmatrix} \mathbf{K}_i & \mathbf{C}_i^T \\ \mathbf{C}_i & \mathbf{0} \end{bmatrix} \begin{bmatrix} \mathbf{u}_i \\ \mu_i \end{bmatrix} = \begin{bmatrix} \mathbf{R}_{Bi}^T \mathbf{D}_i \mathbf{R}_i^\Gamma \mathbf{r}^\Gamma \\ \mathbf{0} \end{bmatrix}, \quad i = 1, \dots, N_S,$$

where \mathbf{K}_C is the stiffness matrix of the global coarse problem, \mathbf{K}_i is the local matrix assembled from elements in the i -th subdomain, and \mathbf{C}_i is a constraint matrix enforcing zero values of the local coarse degrees of freedom in the second block row of (3.9). The restriction matrix \mathbf{R}_{Bi} selects the local interface unknowns from those at the whole subdomain, the columns of Φ_i contain the local coarse basis functions, and \mathbf{R}_{Ci} is the restriction matrix of the global vector of coarse unknowns to those present at the i -th subdomain.

Matrix \mathbf{D}_i applies weights to satisfy the partition of unity. In this work, it corresponds to a diagonal matrix with entries given either by the inverse cardinality of the set of subdomains sharing the interface unknown (denoted as *card*) or derived from the diagonal entries of the local stiffness matrices (denoted as *diag*). These are rather standard choices in the DD literature (see, e.g., [26]).

When the number of subdomains reaches thousands, scalable solution of problem (3.8) by a direct solver becomes a challenge [1, 24]. A way to overcome this issue is to solve the coarse problem only approximately. In multilevel BDDC [27, 17], we apply the preconditioner to the coarse problem with subdomains playing the role of elements. Details of our implementation within the BDDCML library can be found in [24].

3.3. Adaptive selection of coarse degrees of freedom. The idea of adaptive BDDC is to enrich the coarse space by additional degrees of freedom. These are

chosen so that the condition number of the preconditioned operator $\kappa(\mathbf{M}_{BDDC}^{-1}\mathbf{A})$ is reduced in a close-to-optimal way. In the present work, we apply the method described in [16, 18, 15]. It is combined with the three-level BDDC preconditioner as a special case of adaptive multilevel BDDC [24]. Although adaptive BDDC was developed for problems requiring a large number of iterations such as those with jumps in material parameters, the studied problem presents another potential use case in which strengthening the preconditioner at the cost of additional computations in its setup may lead to reduction of the overall number of iterations and, ultimately, the computational time.

In adaptive BDDC, a number of generalized eigenvalue problems are solved, each corresponding to a pair of subdomains sharing a face. Suppose that a face is shared by the s -th and the t -th subdomain. The related generalized eigenvalue problem reads

$$(3.10) \quad \mathbf{\Pi}(\mathbf{I} - \mathbf{E}_{st})^T \mathbf{A}_{st}(\mathbf{I} - \mathbf{E}_{st}) \mathbf{\Pi} \mathbf{w} = \lambda \mathbf{\Pi} \mathbf{A}_{st} \mathbf{\Pi} \mathbf{w},$$

where \mathbf{A}_{st} is a block-diagonal matrix composed of the local Schur complements of the s -th and the t -th subdomain,

$$(3.11) \quad \mathbf{A}_{st} = \begin{bmatrix} \mathbf{A}_s & \\ & \mathbf{A}_t \end{bmatrix},$$

$\mathbf{\Pi}$ is a projection matrix enforcing continuity of the coarse degrees of freedom initially defined on the subdomains, such as arithmetic averages on edges and faces of the subdomains, \mathbf{I} is the identity matrix, and \mathbf{E}_{st} is the averaging matrix that makes the unknowns at the common interface continuous.

Once the generalized eigenvalue problems are solved for each pair of subdomains sharing a face, each eigenvector corresponding to an eigenvalue larger than a prescribed threshold τ is used to enrich the coarse space. In particular, if $\lambda_\ell > \tau$, its corresponding eigenvector \mathbf{w}_ℓ is used to define a coarse degree of freedom \mathbf{c}_ℓ^{st} as

$$(3.12) \quad \mathbf{c}_\ell^{st} = \mathbf{w}_\ell^T \mathbf{\Pi}(\mathbf{I} - \mathbf{E}_{st})^T \mathbf{A}_{st}(\mathbf{I} - \mathbf{E}_{st}) \mathbf{\Pi}.$$

The part of the vector \mathbf{c}_ℓ^{st} that corresponds to the unknowns within a face between the subdomains is added as a new row into the matrices \mathbf{C}_s and \mathbf{C}_t from the respective problems (3.8). Details of the employed approach can be found in [24].

The prescribed threshold $\tau > 1$ is an approximation of the target condition number of the preconditioned system $\kappa(\mathbf{M}_{BDDC}^{-1}\mathbf{A})$. The smaller the threshold, the more coarse degrees of freedom are added. This has the effect of reducing the number of iterations at the cost of increasing the size of the global coarse problem, and hence the cost of each action of the BDDC preconditioner. Consequently, there is a trade-off between pushing the number of iterations down and the cost of each of them in adaptive BDDC. It should be also noted that although the solution of the local generalized eigenvalue problems is parallelized, it still presents a significant overhead in the setup of the BDDC preconditioner that is realized before solving the problem in the first time step.

4. Stopping criteria based on (algebraic) residual. A common (often the default) criterion to terminate an iterative solver is a prescribed reduction of the relative residual. More precisely, a criterion like

$$(4.1) \quad \frac{\|\mathbf{r}_k\|}{\|\mathbf{r}_0\|} < tol$$

is considered, where \mathbf{r}_k is the residual in the k -th iteration, $\mathbf{r}_k = \mathbf{b} - \mathbf{A}\mathbf{x}_k$, and \mathbf{r}_0 is the residual associated with the initial guess \mathbf{x}_0 . The key benefit of this criterion is that it involves only (cheaply) computable quantities. On the other hand, one should be aware of its significant limitations:

1. For ill-conditioned systems, a small residual norm does not guarantee a small norm of the error. Recall the well-known relationship

$$\frac{\|\mathbf{x} - \mathbf{x}_k\|}{\|\mathbf{x}\|} \leq \kappa(\mathbf{A}) \frac{\|\mathbf{r}_k\|}{\|\mathbf{b}\|},$$

where $\kappa(\mathbf{A})$ is the condition number of matrix \mathbf{A} (with respect to a $\|\cdot\|$ norm). This bound is sharp, meaning that there exist an approximation \mathbf{x}_k and the associated residual \mathbf{r}_k such that it holds with the equality.

2. The norm $\|\mathbf{r}_k\|$ depends on the discretization basis and has no continuous counterpart, i.e., it is not equal to a norm of some continuous function.
3. It is not clear how to choose the tolerance tol in (4.1).

A use of an efficient preconditioner, which is our case, resolves the first point raised above and partially also the second one; preconditioned residual is close to the error for very well-conditioned systems. Nevertheless, setting properly the tolerance is a challenging issue that is a subject of our future work. We expect that it should be based on a posteriori error estimates for errors due to the discretization and linearization of (2.1). In this work, we use a common choice $tol = 10^{-6}$.

There is another good reason why (4.1) may be a bad choice when solving sequences of linear systems. An accurate approximation $\mathbf{x}_0 \approx \mathbf{x}$ (for example by using the approximation computed for the previous system) typically makes the norm of the initial residual \mathbf{r}_0 small. The requirement of further improving the norm of the residual \mathbf{r}_k by several orders of magnitude then may lead to useless iterations and an effect of *over-solving*; after certain level, the error in computing $\psi^{(n+1)}$ in (2.3) is dominated by the FEM discretization error and reducing the algebraic error further brings no improvement. Consequently, it is important to normalize $\|\mathbf{r}_k\|$ by a quantity that is not related to the initial approximation. In this study, we take the norm of the right-hand side vector \mathbf{b} for this purpose, and we terminate the iterations when

$$(4.2) \quad \frac{\|\mathbf{r}_k\|}{\|\mathbf{b}\|} < 10^{-6}.$$

It seems essential to combine the choice of the non-zero initial solution \mathbf{x}_0 with this stopping criterion in order to achieve the reduction of the number of iterations expected from an accurate initial guess. Especially for problems that converge (with increasing time) to a particular solution and hence the subsequent algebraic systems become progressively closer to each other.

Finally, note that (4.2) is used as a stopping criterion for PCG for example in MATLAB R2019b, SciPy (all versions), or PETSc 3.21. However, (4.1) was the default option in PETSc until the 3.18 release, and it might still be used in some other software.

5. Krylov subspace recycling. The principle of deflation for iterative solvers starts with decomposing the solution space \mathbb{R}^n as $\mathbb{R}^n = \mathcal{U} + \mathcal{V}$, where \mathcal{U} is a *deflation* subspace of a (relatively) small dimension, and \mathcal{V} is the orthogonal complement of \mathcal{U} with respect to a suitable inner product. Then the given problem is solved directly on

\mathcal{U} and iteratively on \mathcal{V} . If the subspace \mathcal{U} is chosen properly, one can get a significant speed-up of the iterative solution.

Deflation brings two challenges: how to construct \mathcal{U} , and how to implement the iterative method on \mathcal{V} . While the latter is a technical issue that has been resolved for many iterative (Krylov) methods and is independent of the choice of \mathcal{U} (and \mathcal{V}), a proper choice of the deflation subspace is problem-dependent and should be carefully addressed for each application.

In this section, we first recall the deflated preconditioned conjugate gradient method following the original literature [20, 8, 22]. Then we present the choice of the deflation space that is, in our case, based on subspace recycling from [22] with certain modifications.

5.1. Deflated preconditioned conjugate gradient method. For a square matrix $\mathbf{A} \in \mathbb{R}^{n \times n}$ and a vector $\mathbf{v} \in \mathbb{R}^n$, define the j -th Krylov subspace

$$\mathcal{K}_j(\mathbf{A}, \mathbf{v}) = \text{span}\{\mathbf{v}, \mathbf{A}\mathbf{v}, \dots, \mathbf{A}^{j-1}\mathbf{v}\}.$$

Given a symmetric positive definite matrix \mathbf{A} , a right-hand side \mathbf{b} , and an initial approximation \mathbf{x}_0 , define the initial residual $\mathbf{r}_0 = \mathbf{b} - \mathbf{A}\mathbf{x}_0$. In the j -th iteration, CG generates an approximation \mathbf{x}_j characterized by

$$\mathbf{x}_j \in \mathbf{x}_0 + \mathcal{K}_j(\mathbf{A}, \mathbf{r}_0), \quad \mathbf{r}_j = \mathbf{b} - \mathbf{A}\mathbf{x}_j \perp \mathcal{K}_j(\mathbf{A}, \mathbf{r}_0)$$

The implementation of CG can be found, e.g., in the seminal paper [12].

Let us store basis vectors of the subspace \mathcal{U} as columns of matrix \mathbf{W} . Define

$$(5.1) \quad \mathbf{Q} = \mathbf{I} - \mathbf{W}(\mathbf{W}^T \mathbf{A} \mathbf{W})^{-1} \mathbf{W}^T \mathbf{A},$$

and, for \mathbf{v} such that $\mathbf{W}^T \mathbf{v} = 0$,

$$\mathcal{K}_{\mathcal{U},j}(\mathbf{A}, \mathbf{v}) = \mathcal{U} + \mathcal{K}_j(\mathbf{Q}\mathbf{A}\mathbf{Q}, \mathbf{v}).$$

Here \mathbf{Q} is a projector on \mathcal{V} , which is an orthogonal complement of \mathcal{U} with respect to the inner product induced by matrix \mathbf{A} . Therefore, $\mathcal{K}_j(\mathbf{Q}\mathbf{A}\mathbf{Q}, \mathbf{v}) \cap \mathcal{U} = \{0\}$. Deflated Conjugate Gradient method is a modification of CG that generates approximations such that

$$\mathbf{x}_j \in \mathbf{x}_0 + \mathcal{K}_{\mathcal{U},j}(\mathbf{A}, \mathbf{r}_0), \quad \mathbf{r}_j = \mathbf{b} - \mathbf{A}\mathbf{x}_j \perp \mathcal{K}_{\mathcal{U},j}(\mathbf{A}, \mathbf{r}_0),$$

assuming that \mathbf{x}_0 is such that $\mathbf{W}^T \mathbf{r}_0 = 0$. A corresponding algorithm is given in [22, Algorithm 3.5]; see also [8, Sect. 3]. For the ease of presentation, we will call \mathbf{W} the deflation basis.

To speed up the convergence of CG (or any iterative method in general), a suitable preconditioning formally transforming the problem $\mathbf{A}\mathbf{x} = \mathbf{b}$ into $\mathbf{M}^{-1}\mathbf{A}\mathbf{x} = \mathbf{M}^{-1}\mathbf{b}$ is often considered. Preconditioning can be also used in combination with the deflation. The corresponding algorithm is given, e.g., in [22, Algorithm 3.6], and we provide it below as [Algorithm 5.1](#) for completeness.

In comparison with the standard PCG, deflated PCG additionally requires a computation of initial vector \mathbf{x}_0 from \mathbf{x}_{-1} (line 3 of [Algorithm 5.1](#)) and a projection of \mathbf{z}_0 onto \mathcal{V} , $\mathbf{p}_0 = \mathbf{Q}\mathbf{z}_0 = (\mathbf{I} - \mathbf{W}(\mathbf{W}^T \mathbf{A} \mathbf{W})^{-1} \mathbf{W}^T \mathbf{A})\mathbf{z}_0$ (lines 6 and 7 of [Algorithm 5.1](#)) in the initial setup. These operations require solution of a system with the matrix $\mathbf{W}^T \mathbf{A} \mathbf{W}$, which has the size equal to the dimension of the deflation space. Then another projection $\mathbf{Q}\mathbf{z}_j = (\mathbf{I} - \mathbf{W}(\mathbf{W}^T \mathbf{A} \mathbf{W})^{-1} \mathbf{W}^T \mathbf{A})\mathbf{z}_j$ must be additionally computed in each iteration (lines 15 and 16 of [Algorithm 5.1](#)). These operations and the

Algorithm 5.1 Deflated PCG

```

1: let  $\mathbf{W} = [\mathbf{w}_1, \mathbf{w}_2, \dots, \mathbf{w}_k]$  be a basis of  $\mathcal{U}$ 
2: input  $\mathbf{A}$ ,  $\mathbf{b}$ , preconditioner  $\mathbf{M}$ , initial guess  $\mathbf{x}_{-1}$ 
3:  $\mathbf{x}_0 = \mathbf{x}_{-1} + \mathbf{W}(\mathbf{W}^T \mathbf{A} \mathbf{W})^{-1} \mathbf{W}^T (\mathbf{b} - \mathbf{A} \mathbf{x}_{-1})$            to assure that  $\mathbf{W}^T \mathbf{r}_0 = 0$ 
4:  $\mathbf{r}_0 = \mathbf{b} - \mathbf{A} \mathbf{x}_0$ 
5:  $\mathbf{z}_0 = \mathbf{M}^{-1} \mathbf{r}_0$ 
6:  $\hat{\mu}_0 = (\mathbf{W}^T \mathbf{A} \mathbf{W})^{-1} \mathbf{W}^T \mathbf{A} \mathbf{z}_0$ 
7:  $\mathbf{p}_0 = \mathbf{z}_0 - \mathbf{W} \hat{\mu}_0$            equivalently  $\mathbf{p}_0 = (\mathbf{I} - \mathbf{W}(\mathbf{W}^T \mathbf{A} \mathbf{W})^{-1} \mathbf{W}^T \mathbf{A}) \mathbf{z}_0$ 
8: for  $j = 1, 2, \dots$  until convergence do
9:    $\alpha_{j-1} = \mathbf{r}_{j-1}^T \mathbf{z}_{j-1} / \mathbf{p}_{j-1}^T \mathbf{A} \mathbf{p}_{j-1}$ 
10:   $\mathbf{x}_j = \mathbf{x}_{j-1} + \alpha_{j-1} \mathbf{p}_{j-1}$ 
11:   $\mathbf{r}_j = \mathbf{r}_{j-1} - \alpha_{j-1} \mathbf{A} \mathbf{p}_{j-1}$ 
12:   $\mathbf{r}_j = \mathbf{r}_j - \mathbf{W}(\mathbf{W}^T \mathbf{W})^{-1} \mathbf{W}^T \mathbf{r}_j$ 
13:   $\mathbf{z}_j = \mathbf{M}^{-1} \mathbf{r}_j$ 
14:   $\beta_{j-1} = \mathbf{r}_j^T \mathbf{z}_j / \mathbf{r}_{j-1}^T \mathbf{z}_{j-1}$ 
15:   $\hat{\mu}_j = (\mathbf{W}^T \mathbf{A} \mathbf{W})^{-1} \mathbf{W}^T \mathbf{A} \mathbf{z}_j$ 
16:   $\mathbf{p}_j = \mathbf{z}_j + \beta_{j-1} \mathbf{p}_{j-1} - \mathbf{W} \hat{\mu}_j$     $\mathbf{p}_j = \beta_{j-1} \mathbf{p}_{j-1} + (\mathbf{I} - \mathbf{W}(\mathbf{W}^T \mathbf{A} \mathbf{W})^{-1} \mathbf{W}^T \mathbf{A}) \mathbf{z}_j$ 
17: end for

```

need of storing the basis \mathbf{W} increase the time and memory requirements of deflated PCG. Hence, similarly to adaptive BDDC, the deflation leads to a trade-off between reducing the number of iterations and increasing their cost.

Mathematically, it holds that $\mathbf{W}^T \mathbf{r}_j = \mathbf{W}^T \mathbf{p}_j = 0$. In finite-precision computations, however, this may not hold due to the loss of orthogonality. In such cases, the reorthogonalization of residuals at line 12 of Algorithm 5.1 may be necessary; see also [22, Eq. (7.1)].

5.2. Subspace recycling. To construct a deflation space \mathcal{U} , one can use some a priori information on the eigenvector spaces corresponding to a problematic part of the spectrum, as was considered, e.g., in [8]. However, we have no such information in hand for the considered application.

When solving a sequence of systems $\mathbf{A} \mathbf{x}^{(i)} = \mathbf{b}^{(i)}$, the idea might be to reuse, or *recycle*, the Krylov subspace built for the previous system(s) to construct the deflation space for the current system. We denote the vectors computed in (deflated) PCG applied to $\mathbf{A} \mathbf{x}^{(i)} = \mathbf{b}^{(i)}$ by the superscript, for example $\mathbf{p}_j^{(i)}$ denotes the j -th search vector for the i -th system. The maximal dimension of the deflation space is a parameter to be chosen by the user, we denote it by R .

In the experiments, we first test two simple constructions of the deflation basis:

B1 (first R search vectors). The deflation basis is set as the first R search vectors and then remains unchanged for the rest of the computation, $\mathbf{W}^{(i)} = \mathbf{W} = [\mathbf{p}_1^{(1)}, \mathbf{p}_2^{(1)}, \dots, \mathbf{p}_R^{(1)}]$. If R is larger than the number ℓ of PCG iterations for solving the first system, the basis \mathbf{W} also contains the search vectors from solving the second system (and possibly more systems until it has R columns), $\mathbf{W} = [\mathbf{p}_1^{(1)}, \dots, \mathbf{p}_\ell^{(1)}, \mathbf{p}_1^{(2)}, \dots]$.

B2 (last R search vectors). The basis is first constructed as in the previous case, and then it uses a ‘sliding window’ to contain the last R search vectors from the previous systems. This choice is motivated by the fact that the search vectors from the preceding linear systems may be more relevant to the subsequent system to be solved. In more detail, after solving the $(i-1)$ -th system and saving ℓ search vectors

as columns of $\mathbf{P}^{(i-1)}$, the deflation basis is updated as

$$\mathbf{W}^{(i)} = \left[\mathbf{w}_{\ell+1}^{(i-1)}, \mathbf{w}_{\ell+2}^{(i-1)}, \dots, \mathbf{w}_R^{(i-1)}, \mathbf{p}_1^{(i-1)}, \mathbf{p}_2^{(i-1)}, \dots, \mathbf{p}_\ell^{(i-1)} \right].$$

In other words, ℓ ‘oldest’ vectors in $\mathbf{W}^{(i-1)}$ are replaced by the most recent search vectors while keeping the number of columns of \mathbf{W} equal to R .

The search vectors \mathbf{p}_j are in PCG, as well as in deflated PCG ([22, Prop. 3.3]), \mathbf{A} -orthogonal, $\mathbf{p}_j^T \mathbf{A} \mathbf{p}_l = 0$ for $j \neq l$. Therefore, if the basis \mathbf{W} contains the search vectors only, the matrix $\mathbf{W}^T \mathbf{A} \mathbf{W}$ is diagonal and the projection \mathbf{Q} in (5.1) only consists of matrix multiplications. In finite-precision computations, the \mathbf{A} -orthogonality between the search vectors is often lost during the course of iterations. However, in our application with the BDDC preconditioner, only a decent number of PCG iteration was needed to reach the tolerance, and the loss of orthogonality was modest in our experiments.

The choice of the deflation basis according to *B1* and *B2* allows for a cheaper (faster) iterations, but the overall speed-up can be higher for the more elaborated construction of the deflation space from [22]. In particular, the construction is based on storing (some of) the search direction vectors and determining the new basis $\mathbf{W}^{(i)}$ as the solution of an eigenvalue problem. Note that such a basis is not necessarily \mathbf{A} -orthogonal, and consequently, matrix $\mathbf{W}^T \mathbf{A} \mathbf{W}$ is no longer diagonal. This recycling procedure is as follows:

1. Solve the first system $\mathbf{A} \mathbf{x}^{(1)} = \mathbf{b}^{(1)}$. Save (some of) the search vectors $\mathbf{p}_j^{(1)}$ computed within the PCG iterations into the matrix $\mathbf{P}^{(1)}$ and the associated vectors $\mathbf{A} \mathbf{p}_j^{(1)}$ into $\mathbf{A} \mathbf{P}^{(1)}$. The maximum number of vectors to save is, in general, one of the parameters to be determined by the user. We use all search vectors from each PCG run in this paper. Set $\mathbf{W}^{(1)} = \emptyset$.
2. For the other systems in the sequence, $i = 2, 3, \dots, n_i$:
 - (a) Use vectors in $\mathbf{W}^{(i-1)}$, $\mathbf{P}^{(i-1)}$, and $\mathbf{A} \mathbf{P}^{(i-1)}$ to generate a generalized eigenvalue problem specified below.
 - (b) Solve the eigenvalue problem and determine matrix $\mathbf{W}^{(i)}$ using a part of the computed eigenvectors. These vectors ideally approximate some eigenvectors of $\mathbf{M}^{-1} \mathbf{A}$.
 - (c) Solve $\mathbf{A} \mathbf{x}^{(i)} = \mathbf{b}^{(i)}$ by deflated PCG with an initial guess $\mathbf{x}_{-1}^{(i)}$, preconditioner \mathbf{M}^{-1} , and the deflation space basis $\mathbf{W}^{(i)}$. As for the first system, construct successively the matrices $\mathbf{P}^{(i)}$ and $\mathbf{A} \mathbf{P}^{(i)}$.

It remains to detail how the generalized eigenvalue problem is constructed. The information in $\mathbf{W}^{(i-1)}$ and $\mathbf{P}^{(i-1)}$ is combined to improve the approximation to the eigenvectors of the preconditioned matrix $\mathbf{M}^{-1} \mathbf{A}$. Denote by \mathbf{V} the concatenated matrix $\mathbf{V} = [\mathbf{W}^{(i-1)}, \mathbf{P}^{(i-1)}]$, then the *Ritz approximation* to the eigenpairs of $\mathbf{M}^{-1} \mathbf{A}$ is given by solving

$$(5.2) \quad \mathbf{V}^T \mathbf{A} \mathbf{V} \mathbf{y} = \theta \mathbf{V}^T \mathbf{M} \mathbf{V} \mathbf{y}$$

and setting $\mathbf{w} = \mathbf{V} \mathbf{y}$ as an approximation to an eigenvector of $\mathbf{M}^{-1} \mathbf{A}$. This standard approximation, however, requires to apply the preconditioner \mathbf{M} to \mathbf{V} , which may not be possible when only the operation $\mathbf{M}^{-1} \mathbf{v}$ is available, as in our case of the BDDC preconditioner. As in [22, Sect. 5.1], we therefore consider the *harmonic Ritz approximation*

$$(5.3) \quad \mathbf{V}^T \mathbf{A} \mathbf{M}^{-1} \mathbf{A} \mathbf{V} \mathbf{y} = \theta \mathbf{V}^T \mathbf{A} \mathbf{V} \mathbf{y}$$

that involves the operation with the inverse of the preconditioner. Moreover, we employ a strategy from [22, Sections 5.1 and 5.2] for constructing matrices $\mathbf{V}^T \mathbf{A} \mathbf{M}^{-1} \mathbf{A} \mathbf{V}$ and $\mathbf{V}^T \mathbf{A} \mathbf{V}$ from (5.3) for $\mathbf{V} = [\mathbf{W}^{(i-1)}, \mathbf{P}^{(i-1)}]$ at a low cost. Notice that while problems (5.2) and (5.3) are different, they both provide approximations to the eigenvalues and eigenvectors of the preconditioned system matrix $\mathbf{M}^{-1} \mathbf{A}$.

After solving one or several systems, the maximal size R of the deflation basis $\mathbf{W}^{(i-1)}$ is reached, and only a subset of R harmonic Ritz approximations (eigenpairs satisfying (5.3) and setting $\mathbf{w} = \mathbf{V} \mathbf{y}$) are taken to form $\mathbf{W}^{(i)}$. We consider two variants:

B3 (eliminating R smallest Ritz values). For $\mathbf{V} = [\mathbf{W}^{(i-1)}, \mathbf{P}^{(i-1)}]$ and \mathbf{y}_l the generalized eigenvector from (5.3) corresponding to the l -th *smallest* Ritz value θ_l , set the deflation vector $\mathbf{w}_l = \mathbf{V} \mathbf{y}_l$, $l = 1, 2, \dots, R$. This choice from [22] is motivated by the fact that the smallest eigenvalues of $\mathbf{M}^{-1} \mathbf{A}$ typically harm the convergence of (deflated) PCG the most.

B4 (eliminating R largest Ritz values). Analogous to *B3*, but now the eigenvectors corresponding to the *largest* Ritz values θ_l are taken to construct \mathbf{w}_l . This is a key modification for our application. Since the BDDC preconditioner shifts the lower part of the spectrum to one, creating a cluster of eigenvalues there, the deflation space would need to be very large to guarantee a faster convergence for *B3*. Despite the fact that also the upper part of the spectrum is close to one (the largest eigenvalues were $O(1)$ in our experiments) and the largest eigenvalues and corresponding eigenspaces are typically implicitly well-approximated by Ritz values and vectors in PCG, this choice for $\mathbf{W}^{(i)}$ gives an interesting speed-up.

Finally, note that after solving some number of systems $\mathbf{A} \mathbf{x}^{(i)} = \mathbf{b}^{(i)}$, the eigenpairs of $\mathbf{M}^{-1} \mathbf{A}$ can be well approximated, and no further improvement is gained by solving (5.3). Therefore, we set a heuristic criterion

$$(5.4) \quad \frac{\|\boldsymbol{\theta}^{(i)} - \boldsymbol{\theta}^{(i-1)}\|_2}{\|\boldsymbol{\theta}^{(i)}\|_2} \leq 10^{-5},$$

where $\boldsymbol{\theta}^{(i)}$ denotes R harmonic Ritz values given by (5.3) for the i -th system and selected according to *B3* or *B4* described above. When criterion (5.4) is satisfied, say after solving the m -th system, the deflation space approximates the space spanned by the R eigenvectors corresponding to the largest (or smallest) eigenvalues sufficiently well, and the basis is fixed for all the subsequent systems, $\mathbf{W}^{(n)} = \mathbf{W}^{(m)}$, $n \geq m$. Criterion (5.4) can be replaced by a more elaborated stopping criteria; see, e.g., [2]. However, (5.4) performs satisfactorily in our computations.

6. Results. In this section, we present numerical results for the simulation of incompressible flow around a unit sphere. We focus on multiple variants of the three-level BDDC method for the Poisson problem for pressure corrector (2.3) with a fixed matrix and time-dependent right-hand side vector. The computational mesh of Taylor–Hood hexahedral elements leads to 1.4M unknowns for pressure, and it is decomposed into 1024 subdomains; see Fig. 1. The time step is set to 0.05 s.

The problems for velocity components (2.2) are solved using GMRES implementation from the PETSc library (version 3.16.3) with the relative residual tolerance set to 10^{-6} . In addition, the problem of the pressure update (2.4) is solved by PCG from PETSc with the relative residual tolerance set also to 10^{-6} .

The computations were performed on the *Karolina* supercomputer at the IT4Innovations National Supercomputing Centre in Ostrava, Czech Republic. The computational nodes are equipped with two 64-core AMD 7H12 2.6 GHz processors, and

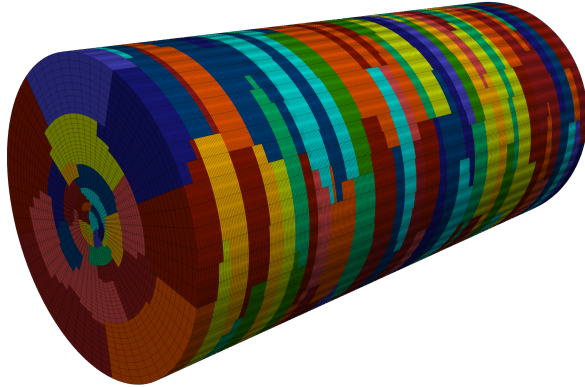


Fig. 1: Computational mesh for the flow around the unit sphere decomposed into 1024 subdomains.

256 GB RAM.

6.1. Effect of the stopping criterion. We consider two Reynolds numbers, 100 and 300, which lead to fundamentally different regimes with respect to the dependence on time. Our main focus is the simulation of the flow at Reynolds number 300. After an initial phase, the solution is periodic, see Fig. 2 for several snapshots of vortex structures in different times and the right part of Fig. 5 for the evolution of the drag and lift coefficients in time. However, we first focus on the choice of the initial guess and the stopping criteria, and for that purpose, it is customary to perform simulations for the case of Reynolds number 100. For this lower Re , the solution is transient, and it converges to a steady state as can be deduced from the plot of the aerodynamic coefficients in Fig. 5. The vortex structure resembles the solution at the second snapshot of Fig. 2. From the linear algebraic viewpoint, the subsequent linear systems (2.5) are becoming closer to each other, and the solution from the preceding time step is a progressively better approximation to the solution from the actual time step. We are interested in the capability of the solver to exploit this fact and converge in a lower number of iterations.

The cumulative number of PCG iterations in 4000 time steps for the different configurations is presented in Fig. 3. We consider the choice of initial guess as the vector of zeros as well as the final approximation computed in the previous time step. Two stopping criteria, (4.1) and (4.2) are compared. The cumulative number illustrates the overall demand for the number of iterations of each approach over the course of the simulation, and it provides an insight into the long-term efficiency of the criterion, here when converging to a stationary solution.

From Fig. 3, we can see that the lines corresponding to starting the solution always with the zero guess overlap (when starting with the zero guess, the stopping criteria (4.1) and (4.2) coincide as $\mathbf{r}_0 = \mathbf{b}$) and show a constant increase, indicating that the number of iterations remains almost constant in each step. When the solver for the new time step starts with the solution from the previous time step and the stopping criterion is based on the norm of the initial residual, there is a slight decrease in the number of iterations, which is approximately constant over the time steps. Even

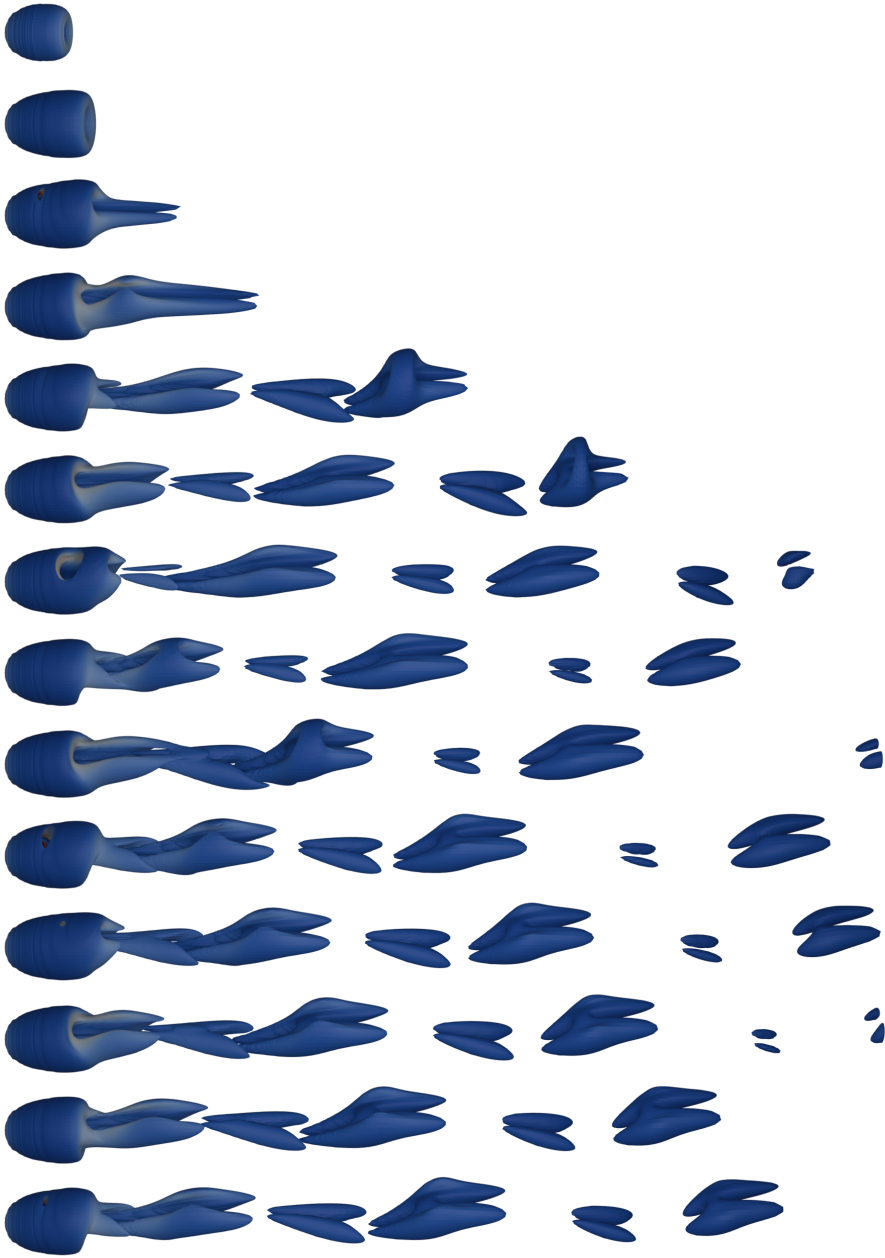


Fig. 2: Vortex structures behind a unit sphere at Re 300 at times 2.5, 25, 45, 50, 60, 65, 71, 75, 80, 100, 125, 150, 175, 200 s.

though the systems are converging to each other, the PCG method with the stopping criterion (4.1) based on the initial residual is not capable of reducing the number of iterations sufficiently during the simulation.

Importantly, this desired behavior is obtained for the stopping criterion (4.2)

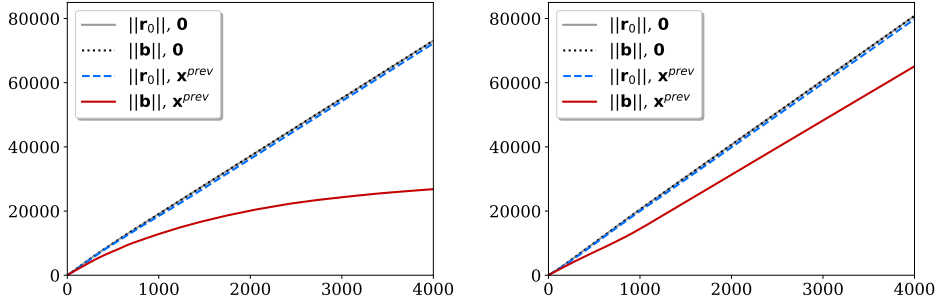


Fig. 3: Cumulative number of PCG iterations over all time steps for $\text{Re} = 100$ (transient solution, left) and $\text{Re} = 300$ (periodic solution, right). Iterations terminated using $\|\mathbf{r}_k\|/\|\mathbf{r}_0\|$ (denoted by ‘ $\|\mathbf{r}_0\|$ ’) and $\|\mathbf{r}_k\|/\|\mathbf{b}\|$ (‘ $\|\mathbf{b}\|$ ’) stopping criteria, initial guess taken as a zero vector (‘ $\mathbf{0}$ ’) and as the approximate solution from the previous time step (‘ \mathbf{x}^{prev} ’).

based on the norm of the right-hand side vector, and the number of iterations decreases during the course of the time steps. As illustrated in the left part of Fig. 3, selecting an appropriate stopping criterion alone can significantly reduce the cumulative number of iterations for a simulation of the transient flow with Reynolds number 100, in our case cutting the computational time by more than 50 percent.

In order to investigate this simulation closer, we present a plot of the residual norms at the beginning and at the end of each time step in Fig. 4. This clearly illustrates that while the residual norm of the initial guess computed from the previous approximation is decreasing in later time steps when the two consecutive solutions get closer to each other, the stopping criterion based on $\|\mathbf{r}_0\|$ leads to significant over-solving. In most of the time steps, the residual norm of initial guesses nearly coincide showing that a softer stopping criterion is sufficient. This is also confirmed when one compares the computed drag and lift coefficients in Fig. 5. The relative difference between the coefficients stays, apart from a few initial time steps, below 10^{-6} indicating that the criterion (4.2) is indeed sufficient.

6.2. Effect of Krylov subspace recycling. In our further experiments, we focus on the case with $\text{Re} = 300$, where a notable change of the regime results in a periodic behavior. In this case, as shown in the right side of Fig. 3, the choice of the initial guess and an appropriate stopping criterion alone does not lead to substantial savings as for $\text{Re} = 100$, although the improvement is still considerable. In the right part of Fig. 4, we can see that in the periodic regime the residual norm of the initial guess computed from the previous approximation does not decrease. After an initial phase (approximately 1000 time steps) where the periodic solution is developed, the initial residual stagnates on a certain level (here around 0.6×10^{-4}). The change in the stopping criterion then allows for a larger residual norm of the computed approximation. This softer criterion leads to a negligible difference in the resulting drag and lift coefficients; see the right panels in Fig. 5.

Let us provide some more quantitative results for $\text{Re} = 300$. In Table 1, we report the minimum, maximum, and mean number of PCG iterations, the mean times for the whole linear solve and for one iteration, and separately the number of iterations

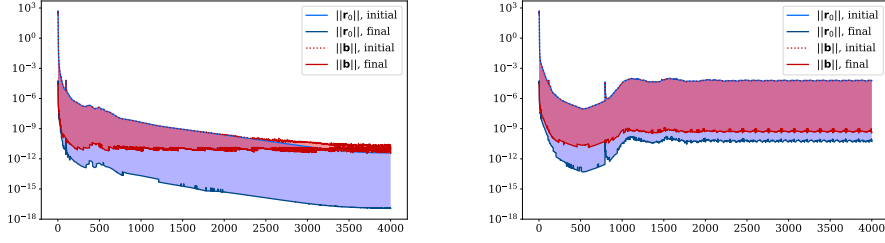


Fig. 4: Norm of the initial and final residual over all time steps for $\text{Re} = 100$ (transient solution, left) and $\text{Re} = 300$ (periodic solution, right). Iterations terminated using $\|\mathbf{r}_k\|/\|\mathbf{r}_0\|$ (denoted as ‘ $\|\mathbf{r}_0\|$ ’) and $\|\mathbf{r}_k\|/\|\mathbf{b}\|$ (‘ $\|\mathbf{b}\|$ ’) stopping criteria.

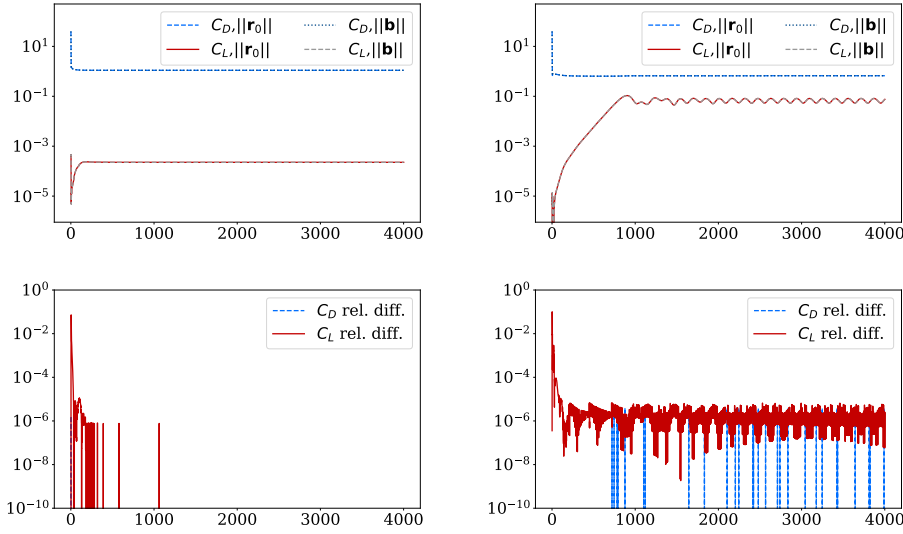


Fig. 5: Drag and lift coefficients over all time steps for $\text{Re} = 100$ (transient solution, top left) and $\text{Re} = 300$ (periodic solution, top right). The bottom panels give the relative difference in the coefficients when computed using the stopping criteria based on $\|\mathbf{r}_k\|/\|\mathbf{r}_0\|$ and $\|\mathbf{r}_k\|/\|\mathbf{b}\|$.

and time for the first step, which is excluded from the other statistics, as it includes the setup of the BDDC preconditioner. For this table (and all tables hereafter), the statistic is computed from the first 100 time steps.

Table 1 confirms that for these simulations, the most beneficial configuration is the variant with the stopping criterion (4.2) based on the norm of the right-hand side vector combined with the computed approximation from the previous time step taken as the initial guess for the new time step. As expected, the mean time for one PCG iteration and the number of iterations for the first step are consistent across all four cases.

In the next experiment, we focus on the strategies for recycling the Krylov sub-

| stop. crit. | init. guess | #its. min-max(avg) | time [s] | step 1 |
|-------------------------------------|----------------------------|-----------------------|---------------|------------------|
| | | | step(1 iter.) | #its. / time [s] |
| $\ \mathbf{r}_k\ /\ \mathbf{r}_0\ $ | $\mathbf{0}$ | 16-22(17.8) | 0.50(0.028) | 23 / 1.56 |
| | \mathbf{x}^{prev} | 16-23(17.2) | 0.48(0.028) | 23 / 1.61 |
| $\ \mathbf{r}_k\ /\ \mathbf{b}\ $ | $\mathbf{0}$ | 16-22(17.8) | 0.49(0.028) | 23 / 1.37 |
| | \mathbf{x}^{prev} | 14-26(15.5) | 0.43(0.028) | 23 / 1.53 |

Table 1: Varying stopping criterion and initial guess, Reynolds number 300: Minimum (‘min’), maximum (‘max’) and mean (‘avg’) number of PCG iterations per time step, mean time for one step with mean time for one iteration in parentheses. For the first step (system), the number of PCG iterations and the overall time including the construction of the BDDC preconditioner are reported.

space. In particular, we consider the four variants of the construction of the deflation basis from Section 5.2 summarized in Table 2 together with four combinations of the stopping criteria and initial guess from the previous experiment. For these simulations, the maximal size of the deflation basis is fixed at $R = 50$. In addition to the results presented in Table 1, we report the time step at which the norm of the Ritz values difference satisfied criterion (5.4). After this step, the deflation basis was not updated.

- B1** (first R search vectors): The deflation basis is kept the same for all systems. It consists of the first R search vectors for the first systems.
- B2** (last R search vectors): The deflation basis consists of the last R search vectors from solving the previous systems.
- B3** (eliminating R smallest Ritz values): The basis contains approximations to R eigenvectors associated with the *smallest* eigenvalues of the preconditioned matrix $\mathbf{M}^{-1}\mathbf{A}$. These are computed using the harmonic Ritz approximation on the subspace generated by the deflation basis (5.3) and the search vectors for the previous system. It is updated in each time step until the criterion (5.4) is satisfied.
- B4** (eliminating R largest Ritz values): Similar to *B3*, but the basis contains approximations associated with the R *largest* eigenvalues of the preconditioned matrix.

Table 2: Summary of the recycling strategies.

From Table 3 we can see that the observation made for the case with no deflation is valid also for these simulations; the most advantageous variant in terms of the number of iterations as well as the time is still the one that uses the stopping criterion (4.2) based on the norm of the right-hand side in combination with taking the solution from the previous time step as the initial guess for the new time step. We observe that the straightforward strategies *B1* and *B2* result in modest savings in both iterations and computational time with *B1* being slightly more efficient.

Note that both *B1* and *B2* slightly outperform *B3* in terms of the average number of iterations. Moreover, *B1* and *B2* do not require recomputing the deflation basis using (5.3). Due to the slow convergence of the smallest Ritz values, the deflation basis is recomputed in each time step when using *B3*.

The best results were obtained for the strategy *B4*, which uses the R vectors

| Recycl. strategy | stop. crit. | init. guess | #its. min-max(avg) | time [s] step(1 iter.) | step 1 | | Ritz conv. |
|------------------|-------------------------------------|--|--------------------|------------------------|-----------|----------|------------|
| | | | | | #its. | time [s] | |
| <i>B1</i> | $\ \mathbf{r}_k\ /\ \mathbf{r}_0\ $ | $\mathbf{0}$ \mathbf{x}^{prev} | 15-24(15.5) | 0.47(0.030) | 23 / 1.49 | n/a | |
| | $\ \mathbf{r}_k\ /\ \mathbf{b}\ $ | $\mathbf{0}$ \mathbf{x}^{prev} | 13-17(15.0) | 0.46(0.031) | 23 / 1.51 | n/a | |
| <i>B2</i> | $\ \mathbf{r}_k\ /\ \mathbf{r}_0\ $ | $\mathbf{0}$ \mathbf{x}^{prev} | 14-24(15.5) | 0.47(0.030) | 23 / 1.71 | n/a | |
| | $\ \mathbf{r}_k\ /\ \mathbf{b}\ $ | $\mathbf{0}$ \mathbf{x}^{prev} | 13-24(13.2) | 0.40(0.031) | 23 / 1.50 | n/a | |
| <i>B3</i> | $\ \mathbf{r}_k\ /\ \mathbf{r}_0\ $ | $\mathbf{0}$ \mathbf{x}^{prev} | 14-17(15.7) | 0.48(0.030) | 23 / 1.71 | n/a | |
| | $\ \mathbf{r}_k\ /\ \mathbf{b}\ $ | $\mathbf{0}$ \mathbf{x}^{prev} | 13-17(15.4) | 0.47(0.030) | 23 / 1.56 | n/a | |
| <i>B3</i> | $\ \mathbf{r}_k\ /\ \mathbf{r}_0\ $ | $\mathbf{0}$ \mathbf{x}^{prev} | 14-17(15.7) | 0.48(0.030) | 23 / 1.48 | n/a | |
| | $\ \mathbf{r}_k\ /\ \mathbf{b}\ $ | $\mathbf{0}$ \mathbf{x}^{prev} | 13-18(13.9) | 0.43(0.031) | 23 / 1.48 | n/a | |
| <i>B3</i> | $\ \mathbf{r}_k\ /\ \mathbf{r}_0\ $ | $\mathbf{0}$ \mathbf{x}^{prev} | 14-19(16.9) | 0.52(0.030) | 23 / 1.74 | >100 | |
| | $\ \mathbf{r}_k\ /\ \mathbf{b}\ $ | $\mathbf{0}$ \mathbf{x}^{prev} | 13-18(16.4) | 0.50(0.030) | 23 / 1.70 | 99 | |
| <i>B3</i> | $\ \mathbf{r}_k\ /\ \mathbf{r}_0\ $ | $\mathbf{0}$ \mathbf{x}^{prev} | 14-19(16.9) | 0.52(0.031) | 23 / 1.78 | >100 | |
| | $\ \mathbf{r}_k\ /\ \mathbf{b}\ $ | $\mathbf{0}$ \mathbf{x}^{prev} | 14-19(14.3) | 0.44(0.031) | 23 / 1.81 | >100 | |
| <i>B4</i> | $\ \mathbf{r}_k\ /\ \mathbf{r}_0\ $ | $\mathbf{0}$ \mathbf{x}^{prev} | 12-16(13.2) | 0.41(0.031) | 23 / 1.81 | 20 | |
| | $\ \mathbf{r}_k\ /\ \mathbf{b}\ $ | $\mathbf{0}$ \mathbf{x}^{prev} | 12-17(12.9) | 0.39(0.031) | 23 / 1.70 | 24 | |
| <i>B4</i> | $\ \mathbf{r}_k\ /\ \mathbf{r}_0\ $ | $\mathbf{0}$ \mathbf{x}^{prev} | 12-16(13.2) | 0.41(0.031) | 23 / 1.69 | 20 | |
| | $\ \mathbf{r}_k\ /\ \mathbf{b}\ $ | $\mathbf{0}$ \mathbf{x}^{prev} | 11-17(11.3) | 0.36(0.031) | 23 / 2.19 | 25 | |

Table 3: Results for different recycling strategies, Reynolds number 300: Minimum (‘min’), maximum (‘max’), and mean (‘avg’) number of PCG iterations per time step, mean time for one time step with mean time for one iteration in parentheses. For the first step, the number of PCG iterations and the overall time including the construction of the BDDC preconditioner are reported. The last column (‘Ritz conv.’) gives the index of the step when the criterion (5.4) is met, i.e., when the Ritz values converged. The size of the deflation basis is set to $R = 50$.

corresponding to the largest Ritz values. This choice requires, on average, the lowest number of PCG iterations, and it requires the lowest computational time for one time step. For this choice, the convergence of the Ritz values over the time steps was relatively fast, and hence the basis was recomputed only in the first few time steps. Following this experiment, we restrict ourselves to the stopping criterion based on the right-hand side vector, previous solution taken as the initial guess, and the recycling strategy *B4* for further experiments.

In the next experiment, we vary the size of the deflation basis R . The results are presented in Table 4. As expected, the mean number of iterations decreases for increasing the size of the deflation basis. However, the time for one iteration increases with increasing R . In fact, the average time for the whole linear solve (i.e., all iterations) and the time step at which the Ritz values converge both reach their minima for the size of the recycling basis $R = 40$, which seems to be the optimal value for this problem and setup. For $R = 50$, used in the previous experiment, the performance is comparable. To provide a fair comparison, we keep the size of the deflation basis $R = 50$ also for the following numerical experiments.

6.3. Effect of adaptive BDDC preconditioner. In the next set of numerical experiments, we perform computations for variants of the adaptive selection of coarse degrees of freedom in the BDDC preconditioner on top of the recycling of the Krylov subspace with $R = 50$. For preliminary results without recycling and with recycling using strategy *B1*, see our paper [11]. In the current experiment, we test several values of the prescribed target value τ from Section 3.3. For a smaller τ , more eigenvectors are used in the coarse problem construction. This reduces the number of iterations, but again, each iteration gets more expensive due to a larger coarse problem. The

| basis size R | #its. | | time [s] | | Ritz conv. |
|-------------------|--------------|---------------|----------------------------|--|---------------|
| | min-max(avg) | step(1 iter.) | step 1 #its. / time [s] | | |
| 25 | 12-19(12.4) | 0.37(0.030) | 23 / 1.86 | | 24 |
| 30 | 12-18(12.3) | 0.36(0.029) | 23 / 1.76 | | 26 |
| 40 | 11-18(11.5) | 0.35(0.031) | 23 / 2.02 | | 20 |
| 50 | 11-17(11.3) | 0.36(0.031) | 23 / 2.19 | | 25 |
| 100 | 9-18(10.7) | 0.38(0.036) | 23 / 1.80 | | 65 |
| 200 | 6-18(8.7) | 0.41(0.044) | 23 / 1.78 | | 89 |
| 400 | 5-18(8.4) | 0.41(0.044) | 23 / 1.94 | | >100 |

Table 4: Varying the maximal size of the recycling basis R : Minimum (‘min’), maximum (‘max’), and mean (‘avg’) number of PCG iterations per time step, mean time for one time step with mean time for one iteration in parentheses. For the first step, the number of PCG iterations and the overall time including the construction of the BDDC preconditioner are reported. The last column (‘Ritz conv.’) gives the index of the step when the criterion (5.4) is met.

method is combined with two types of weights in BDDC (i.e., matrix \mathbf{D}_i introduced in Section 3.2), namely the scaling based on the cardinality (*card*) and based on the diagonal stiffness (*diag*).

| adaptivity weights | | τ | #its. | | time [s] | | step 1 | | Ritz conv. |
|-----------------------|-----|------------|--------------|---------------|------------------|--|--------|----|---------------|
| | | | min-max(avg) | step(1 iter.) | #its. / time [s] | | | | |
| card | 3.5 | 8-14(10.0) | 0.33(0.032) | 17 / 40.88 | | | | 38 | |
| | 3.0 | 9-14(9.4) | 0.31(0.033) | 16 / 40.99 | | | | 85 | |
| | 2.5 | 8-13(9.3) | 0.37(0.040) | 16 / 42.34 | | | | 86 | |
| | 2.0 | 8-13(8.9) | 0.39(0.044) | 15 / 45.16 | | | | 45 | |
| diag | 3.5 | 9-12(9.7) | 0.32(0.033) | 17 / 41.21 | | | | 53 | |
| | 3.0 | 9-12(9.2) | 0.31(0.033) | 17 / 42.44 | | | | 49 | |
| | 2.5 | 9-12(9.2) | 0.31(0.034) | 16 / 42.45 | | | | 34 | |
| | 2.0 | 8-12(8.5) | 0.32(0.037) | 16 / 42.84 | | | | 43 | |

Table 5: Varying the adaptive coarse space in BDDC by changing the threshold on eigenvalues for selecting eigenvectors for the coarse problem τ : Minimum (‘min’), maximum (‘max’), and mean (‘avg’) number of PCG iterations per time step, mean time for one time step with mean time for one iteration in parentheses. The size of the deflation basis $R = 50$. For the first step, the number of PCG iterations and the overall time including the construction of the BDDC preconditioner are reported. The last column (‘Ritz conv.’) gives the index of the step when the criterion (5.4) is met.

From the results in Table 5, we can conclude that the optimal threshold for eigenvalues τ is 3.0 for both types of weights, in terms of both the mean number of iterations and the mean time for the linear solver. The results indicate that the weights based on diagonal stiffness perform slightly better than using cardinality.

It is important to note that, in our current implementation, the adaptive BDDC method introduces a substantial additional cost to the preconditioner setup due to the need to solve the local eigenvalue problems (3.10). By comparing the average time per one time step in Tables 3 and 5, we observe that approximately 500 time steps are needed to amortize this initial cost.

Table 6 presents a summary of the results, comparing the best variant for each

approach. The results show a 23% speed-up for the variant that incorporates both recycling and adaptivity compared to the one without these approaches. To further understand this behavior, Figure 6 displays the Ritz values approximating the spectrum of the preconditioned operator $\mathbf{M}^{-1}\mathbf{A}$, or $\mathbf{QM}^{-1}\mathbf{A}$ when deflation is used, at the 50th time step. The figure illustrates how Krylov subspace recycling and the adaptive BDDC preconditioner push the upper part of the spectrum closer to one, thereby reducing the condition number and accelerating convergence.

| variant | | #its. min-max(avg) | time [s] step(1 iter.) | step 1 | |
|-----------|--------------------|-----------------------|---------------------------|--------|------------|
| recycling | adaptivity | | | #its. | / time [s] |
| ✗ | ✗ | 14-26(15.5) | 0.43(0.028) | 23 | / 1.53 |
| $R = 50$ | ✗ | 11-17(11.3) | 0.36(0.031) | 23 | / 1.70 |
| ✗ | diag, $\tau = 3.0$ | 11-19(11.4) | 0.33(0.030) | 17 | / 45.55 |
| $R = 50$ | diag, $\tau = 3.0$ | 9-12(9.2) | 0.31(0.033) | 17 | / 42.44 |

Table 6: Summary of the best results from Tables 1–5 for different acceleration strategies. Minimum (‘min’), maximum (‘max’), and mean (‘avg’) number of PCG iterations per time step, mean time for one time step with mean time for one iteration in parentheses, and the number of PCG iterations (‘step 1 #its.’), and time for the first time step. We consider the initial guess given by the computed solution to the previous system and the stopping criterion (4.2).

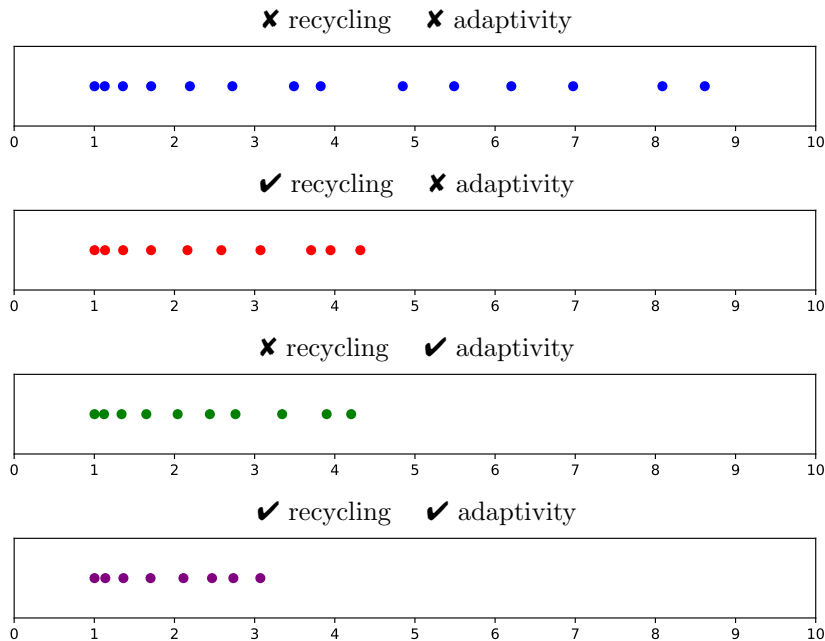


Fig. 6: Ritz values approximating the eigenvalues of the preconditioned system. From top to bottom: no recycling nor adaptive BDDC, Krylov subspace recycling with $R = 50$, no recycling and adaptive BDDC with $\tau = 3.0$, and Krylov subspace recycling with $R = 50$ and adaptive BDDC with $\tau = 3.0$.

To investigate the scalability and efficiency of the acceleration strategies studied

for the smaller mesh size, we finally consider a larger computational mesh, consisting of 15.6 million unknowns for pressure solved on 4096 subdomains and processor cores. We monitor the same metrics of iterations and times as for the smaller problem. Benchmark simulations are carried out again in four different modes: without Krylov subspace recycling, with recycling, with adaptive BDDC, and with a combination of both Krylov subspace recycling and adaptive BDDC. The results are summarized in Table 7.

| variant | | stop. | init. | #its. | time [s] | step 1 | Ritz |
|--------------|--------------|---|----------------------------|--------------|---------------|------------------|-------|
| recycl. | adapt. | crit. | guess | min-max(avg) | step(1 iter.) | #its. / time [s] | conv. |
| \mathbf{x} | \mathbf{x} | $\frac{\ \mathbf{r}_k\ }{\ \mathbf{r}_0\ }$ | $\mathbf{0}$ | 34-47(36.7) | 4.03(0.109) | 47 / 8.55 | n/a |
| | | $\frac{\ \mathbf{r}_k\ }{\ \mathbf{b}\ }$ | \mathbf{x}^{prev} | 34-47(36.0) | 3.98(0.110) | 47 / 8.37 | n/a |
| $R = 50$ | \mathbf{x} | $\frac{\ \mathbf{r}_k\ }{\ \mathbf{r}_0\ }$ | $\mathbf{0}$ | 34-47(36.7) | 3.88(0.106) | 47 / 8.85 | n/a |
| | | $\frac{\ \mathbf{r}_k\ }{\ \mathbf{b}\ }$ | \mathbf{x}^{prev} | 31-54(33.3) | 3.59(0.107) | 47 / 8.24 | n/a |
| $R = 50$ | \mathbf{x} | $\frac{\ \mathbf{r}_k\ }{\ \mathbf{b}\ }$ | \mathbf{x}^{prev} | 22-35(23.3) | 2.67(0.110) | 47 / 8.43 | 18 |
| $R = 50$ | $\tau = 3.0$ | | | 17-30(18.4) | 2.31(0.125) | 26 / 179.86 | n/a |
| $R = 50$ | $\tau = 3.0$ | | | 13-21(14.3) | 1.89(0.132) | 26 / 177.87 | 17 |

Table 7: Larger computational mesh with 15.6 million pressure unknowns: analogy to the results from Tables 1 and 6.

The trends observed for the smaller problem are confirmed for the larger problem; see Table 7. Using the stopping criterion based on the right-hand side vector and initializing the linear solver at each time step with the solution from the previous step results in both the lowest number of iterations and the shortest average time for solving the linear system. When recycling, adaptivity, and their combination are introduced, the results align with those from the smaller problem, but with the differences being more pronounced. The combination of adaptive BDDC and Krylov subspace recycling proves to be the most effective in reducing the iteration count and, more importantly, the computational time for the linear solver. In particular, these acceleration techniques lead to reducing the computational time approximately by 50 %.

Let us also note for completeness that we have performed experiments with different time step sizes, namely, we tested $10\times$ larger and $10\times$ smaller time steps as well. This change had negligible effect on the convergence of the studied Poisson problem of the pressure corrector, and hence the conclusions of the previous experiments remain valid.

7. Conclusions. We have focused on numerical techniques for the solution of time-dependent problems of incompressible flows using time stepping. In particular, we have studied the benchmark problem of flow around a unit sphere with Reynolds numbers 100 and 300. These Reynolds numbers result in fundamentally different regimes with respect to the dependence on time. While for $\text{Re} = 100$, the solution exhibits a transient behaviour converging to a steady solution, the solution for $\text{Re} = 300$ loses stability and becomes periodic in time.

We have applied the incremental pressure-correction method which leads to solving five systems of linear equations in each time step. Out of these, we have focused on the solution of the Poisson problem for pressure corrector which is the most challenging part of the process. From the linear algebraic viewpoint, the problem leads to solving a sequence of algebraic systems with a constant symmetric positive-definite matrix and a right-hand side vector that changes in each time step. Importantly, in

the transient regime for $Re = 100$, the systems within the sequence are getting closer to each other, while this property does not hold for the periodic regime with $Re = 300$.

The systems are solved in parallel using the nonoverlapping domain decomposition method. In particular, we have used the three-level BDDC preconditioner within PCG due to its scalability to very large problems and parallel supercomputers. The standard setting of the three-level BDDC preconditioner provided a baseline for our study, the aim of which has been accelerating the computation across the time steps. Three main algorithmic components have been tested, and their effects on the time-to-solution have been evaluated. First, we explored the effect of initial guess and the stopping criterion. It has been shown that in order to make use of a good initial approximation of the solution, the stopping criterion has to be modified from the usual one based on the initial residual to be independent of the initial guess. In our approach, we have used a stopping criterion normalized by the norm of the right-hand side vector. With this criterion, the Krylov subspace method is capable of decreasing the number of iterations with improving the initial guess, such as using the solution from the previous time step. This capability of the solver turned out to be crucial for saving more than 50 percent of computational time in the transient regime for $Re = 100$.

The second component of the study has been the deflation within PCG combined with Krylov subspace recycling. We have tested four strategies of constructing the deflation basis. Two strategies were based on storing previous search directions, while the other two were based on approximating eigenvectors of the preconditioned system matrix by harmonic Ritz vectors. However, there is a significant difference in our approach from the standard use of the latter. Namely, with a strong preconditioner such as BDDC, the standard approach for deflating the smallest eigenvalues need not work well, and we propose constructing the deflation basis from approximations of the eigenvectors corresponding to the largest eigenvalues. In this regime, the deflation acts as another level of preconditioning, further lowering the upper part of the spectrum of the preconditioned system matrix. The increased cost of each iteration due to the deflation has been compensated by the reduced number of iterations needed to converge.

The last component towards accelerating the method has been the adaptive selection of the coarse space in BDDC. Adaptive BDDC allows to adjust the strength of the preconditioner. Based on solving a number of eigenvalue problems for each pair of subdomains sharing a face, the method constructs a coarse space so that the resulting condition number is approximately bounded by the threshold τ . The smaller the threshold, the more coarse degrees of freedom are defined leading to a smaller number of iterations. However, the cost of solving the coarse problem increases making each iteration more expensive. Due to a significant time spent in the setup of the adaptive BDDC preconditioner, the approach is beneficial for longer runs.

We have shown the synergy of the three approaches for the acceleration of the time-dependent solution. In particular, using the appropriate stopping criteria, previous solution as the initial guess, deflation in the PCG and the adaptive coarse space construction in the multilevel BDDC preconditioner, we have achieved a significant reduction of the computational time. For the transient regime, the reduction was more than one half solely by using the appropriate stopping criterion and more for the other two techniques. For the more challenging problem with the periodic solution, we have saved about one quarter of the computational time for the smaller mesh with 1.4M unknowns for pressure and about one half of the computational time for the larger problem with 15.6M unknowns. Hence, the advanced techniques of Krylov subspace

recycling and adaptive coarse space construction seem to be even more beneficial for more challenging problems which require more PCG iterations for each time step.

Finally, let us mention that there is an optimal size of the deflation basis in the deflated PCG. A similar effect holds for threshold τ within the adaptive BDDC preconditioner. While we have approximately identified these optima in our computations, the results show that these optima are not sharp, and comparable speed-ups can be achieved for a range of values of the parameters. In this sense, the proposed approach seems to be quite robust.

Acknowledgements. This work was supported by the Czech Science Foundation through Grant No. 23-06159S. It was also supported by the Institute of Mathematics of the Czech Academy of Sciences (RVO:67985840). The computational time on the systems at IT4Innovations was provided thanks to the support by the Ministry of Education, Youth and Sports of the Czech Republic through the e-INFRA CZ (ID:90254). The authors would like to thank Žofia Machová for her help with rendering the vortex structures. J. Papež and J. Šístek are members of the Nečas Center for Mathematical Modeling.

REFERENCES

- [1] S. BADIA, A. F. MARTÍN, AND J. PRINCIPE, *Multilevel balancing domain decomposition at extreme scales*, SIAM Journal on Scientific Computing, 38 (2016), pp. C22–C52.
- [2] M. BENNANI AND T. BRACONNIER, *Stopping criteria for eigensolvers*, Tech. Report TR/PA/94/22, CERFACS, 1994.
- [3] N. CHENTANEZ AND M. MÜLLER, *A multigrid fluid pressure solver handling separating solid boundary conditions*, in Proceedings of the 2011 ACM SIGGRAPH/Eurographics Symposium on Computer Animation, SCA '11, New York, NY, USA, 2011, Association for Computing Machinery, pp. 83–90, <https://doi.org/10.1145/2019406.2019418>.
- [4] P. COSTA, *A FFT-based finite-difference solver for massively-parallel direct numerical simulations of turbulent flows*, Computers & Mathematics with Applications, 76 (2018), pp. 1853–1862, <https://doi.org/https://doi.org/10.1016/j.camwa.2018.07.034>.
- [5] C. DICK, M. ROGOWSKY, AND R. WESTERMANN, *Solving the fluid pressure poisson equation using multigrid—evaluation and improvements*, IEEE Transactions on Visualization and Computer Graphics, 22 (2016), pp. 2480–2492, <https://doi.org/10.1109/TVCG.2015.2511734>.
- [6] C. R. DOHRMANN, *A preconditioner for substructuring based on constrained energy minimization*, SIAM Journal on Scientific Computing, 25 (2003), pp. 246–258.
- [7] V. DOLEAN, P. JOLIVET, AND F. NATAF, *An Introduction to Domain Decomposition Methods*, Society for Industrial and Applied Mathematics, Philadelphia, PA, 2015, <https://doi.org/10.1137/1.9781611974065>.
- [8] Z. DOSTÁL, *Conjugate gradient method with preconditioning by projector*, Int. J. Comput. Math., 23 (1988), pp. 315–323, <https://doi.org/10.1080/00207168808803625>.
- [9] G. H. GOLUB, L. C. HUANG, H. SIMON, AND W.-P. TANG, *A fast Poisson solver for the finite difference solution of the incompressible Navier–Stokes equations*, SIAM Journal on Scientific Computing, 19 (1998), pp. 1606–1624, <https://doi.org/10.1137/S1064827595285299>.
- [10] J. L. GUERMOND, P. MINEV, AND J. SHEN, *An overview of projection methods for incompressible flow*, Comput. Methods Appl. Mech. Engrg., 195 (2006), pp. 6011–6045.
- [11] M. HANEK AND J. ŠÍSTEK, *Application of Multilevel BDDC to the problem of pressure in simulations of incompressible flow*, in Domain Decomposition Methods in Science and Engineering XXVI, Lecture Notes in Computational Science and Engineering, S. C. Brenner, E. T. S. Chung, A. Klawonn, F. Kwok, J. Xu, and J. Zou, eds., Springer Cham, 2023, pp. 299–305, https://doi.org/10.1007/978-3-030-95025-5_31.
- [12] M. R. HESTENES AND E. STIEFEL, *Methods of conjugate gradients for solving linear systems*, J. Res. Natl. Bur. Stand., 49 (1952), pp. 409–436, <https://doi.org/10.6028/jres.049.044>.
- [13] R. ISSA, *Solution of the implicitly discretised fluid flow equations by operator-splitting*, Journal of Computational Physics, 62 (1986), pp. 40–65, [https://doi.org/https://doi.org/10.1016/0021-9991\(86\)90099-9](https://doi.org/https://doi.org/10.1016/0021-9991(86)90099-9).
- [14] G. E. KARNIADAKIS, M. ISRAELI, AND S. A. ORSZAG, *High-order splitting methods for the*

- incompressible Navier-Stokes equations*, Journal of Computational Physics, 97 (1991), pp. 414–443, [https://doi.org/https://doi.org/10.1016/0021-9991\(91\)90007-8](https://doi.org/https://doi.org/10.1016/0021-9991(91)90007-8).
- [15] A. Klawonn, M. Kühn, and O. Rheinbach, *Adaptive coarse spaces for FETI-DP in three dimensions*, SIAM J. Sci. Comput., 38 (2016), pp. A2880–A2911, <https://doi.org/10.1137/15M1049610>.
- [16] J. Mandel and B. Soušek, *Adaptive selection of face coarse degrees of freedom in the BDDC and the FETI-DP iterative substructuring methods*, Comput. Methods Appl. Mech. Engrg., 196 (2007), pp. 1389–1399, <https://doi.org/10.1016/j.cma.2006.03.010>.
- [17] J. Mandel, B. Soušek, and C. R. Dohrmann, *Multispace and multilevel BDDC*, Computing, 83 (2008), pp. 55–85.
- [18] J. Mandel, B. Soušek, and J. Šístek, *Adaptive BDDC in three dimensions*, Math. Comput. Simulat., 82 (2012), pp. 1812–1831, <https://doi.org/10.1016/j.matcom.2011.03.014>.
- [19] A. McAdams, E. Sifakis, and J. Teran, *A parallel multigrid poisson solver for fluids simulation on large grids*, in Proceedings of the 2010 ACM SIGGRAPH/Eurographics Symposium on Computer Animation, SCA '10, Goslar, DEU, 2010, Eurographics Association, pp. 65–74.
- [20] R. A. Nicolaides, *Deflation of conjugate gradients with applications to boundary value problems*, SIAM J. Numer. Anal., 24 (1987), pp. 355–365, <https://doi.org/10.1137/0724027>.
- [21] C. Pechstein and C. R. Dohrmann, *A unified framework for adaptive BDDC*, Electron. Trans. Numer. Anal., 46 (2017), pp. 273–336.
- [22] Y. Saad, M. Yeung, J. Erhel, and F. Guyomarc'h, *A deflated version of the conjugate gradient algorithm*, SIAM Journal on Scientific Computing, 21 (2000), pp. 1909–1926, <https://doi.org/10.1137/S1064829598339761>.
- [23] J. Šístek and F. Čížek, *Parallel iterative solution of the incompressible Navier-Stokes equations with application to rotating wings*, Comput. Fluids, 122 (2015), pp. 165–183.
- [24] B. Soušek, J. Šístek, and J. Mandel, *Adaptive-Multilevel BDDC and its parallel implementation*, Computing, 95 (2013), pp. 1087–1119.
- [25] J. M. Tang, S. P. MacLachlan, R. Nabben, and C. Vuić, *A comparison of two-level preconditioners based on multigrid and deflation*, SIAM J. Matrix Anal. Appl., 31 (2010), pp. 1715–1739, <https://doi.org/10.1137/08072084X>.
- [26] A. Toselli and O. B. Widlund, *Domain Decomposition Methods—Algorithms and Theory*, vol. 34 of Springer, Springer-Verlag, 2005.
- [27] X. Tu, *Three-level BDDC in three dimensions*, SIAM Journal on Scientific Computing, 29 (2007), pp. 1759–1780.
- [28] H. G. Weller, G. Tabor, H. Jasak, and C. Fureby, *A tensorial approach to computational continuum mechanics using object-oriented techniques*, Computer in Physics, 12 (1998), pp. 620–631, <https://doi.org/10.1063/1.168744>.